Global Biogeochemical Cycles

RESEARCH ARTICLE
10.1029/2019GB006510

Trace Metal Fractional Solubility in Size-Segregated Aerosols From the Tropical Eastern Atlantic Ocean

Alex R. Baker[1], **Mingpei Li**[1,2], **and Rosie Chance**[1,3]

[1]Centre for Ocean and Atmospheric Science, School of Environmental Sciences, University of East Anglia, Norwich, UK, [2]Now at Interdisciplinary Computing and Complex Biosystems, Newcastle University upon Tyne, Newcastle upon Tyne, UK, [3]Now at Wolfson Atmospheric Chemistry Laboratories, Department of Chemistry, University of York, York, UK

Key Points:
- The solubility in fine fractions of Saharan dust aerosols is enhanced for Fe, Al, and Ti but not for Mn, Co, and Th
- Fe, Al, and Ti solubility increases strongly during atmospheric transport of dust, while Mn, Co, and Th solubility does not
- The stability of Th solubility during transport may make it a more suitable tracer for dust inputs to the ocean than Al or Ti

Supporting Information:
- Supporting Information S1

Correspondence to:
A. R. Baker,
alex.baker@uea.ac.uk

Citation:
Baker, A. R., Li, M., & Chance, R. (2020). Trace metal fractional solubility in size-segregated aerosols from the tropical eastern Atlantic Ocean. *Global Biogeochemical Cycles*, *34*, e2019GB006510. https://doi.org/10.1029/2019GB006510

Received 19 DEC 2019
Accepted 2 MAY 2020

Abstract Soluble and total trace metals were measured in four size fractionated aerosol samples collected over the tropical eastern Atlantic Ocean. In samples that were dominated by Saharan dust, the size distributions of total iron, aluminum, titanium, manganese, cobalt, and thorium were very similar to one another and to the size distributions of soluble manganese, cobalt, and thorium. Finer particle sizes (< ~3 μm) showed enhanced soluble concentrations of iron, aluminum, and titanium, possibly as a result of interactions with acidic sulfate aerosol during atmospheric transport. The difference in fine particle solubility between these two groups of elements might be related to the hyperbolic increase in the fractional solubility of iron, and a number of other elements, during the atmospheric transport of Saharan dust, which is not observed for manganese and its associated elements. In comparison to elements whose solubility varies during atmospheric transport, the stability of thorium fractional solubility should reduce uncertainties in the use of dissolved concentrations of this element in seawater as a proxy for dust deposition, although this topic requires further work.

1. Introduction

Atmospheric deposition of mineral dust is an important source of trace elements to the remote surface ocean. Many of these trace elements (e.g., iron (Fe), phosphorus (P), cobalt (Co), manganese (Mn), and copper (Cu)) are essential components of marine microbial metabolic systems (Mahowald et al., 2018), and thus, the deposition of dust plays a significant role in phytoplankton growth and the cycling of carbon in the ocean and the Earth System as a whole (Jickells et al., 2005).

The solubility (the fraction of their total atmospheric input that dissolves) of these trace elements is key to their impact on microorganisms, because in most cases it is soluble forms that are available for incorporation into cells (e.g., Morel et al., 2008). There is a large body of evidence that indicates that the solubility of Fe increases hyperbolically as total Fe atmospheric concentration decreases (i.e., with transport away from dust source regions) (Baker & Jickells, 2006; Chen & Siefert, 2004; Jickells et al., 2016; Shelley et al., 2018; Sholkovitz et al., 2012). Similar hyperbolic relationships between solubility and atmospheric concentration have been reported for many other dust-associated elements, for example, aluminum (Al), silicon (Si), P, titanium (Ti), and lead (Pb) (Baker & Jickells, 2006; Prospero et al., 1987; Shelley et al., 2018).

Attempts to understand this solubility behavior have focused largely on Fe (Aguilar-Islas et al., 2010; Baker & Jickells, 2006; Sedwick et al., 2007; Sholkovitz et al., 2012; Spokes et al., 1994), because of its major role as a limiting nutrient over large regions of the global ocean (Jickells et al., 2005). Consideration of additional trace elements can help to evaluate the relative importance of potential controls on solubility (Baker et al., 2014), as well as shed light on the biogeochemical cycles of these other species. When trace elements delivered with dust (such as Al, Ti, and thorium (Th)) do not have a significant metabolic function or other confounding factor, their surface water-dissolved concentrations can be used to estimate dust flux and hence the atmospheric supply of associated bioactive elements (Anderson et al., 2016). The fractional solubility of these tracer elements in dust is a key uncertainty in these calculations (Anderson et al., 2016; Hsieh et al., 2011; Measures et al., 2010).

Not all elements exhibit significant increases in solubility with decreasing atmospheric dust concentration. The solubility of Mn in Saharan dust aerosols has been reported to vary little with dust (total Mn)

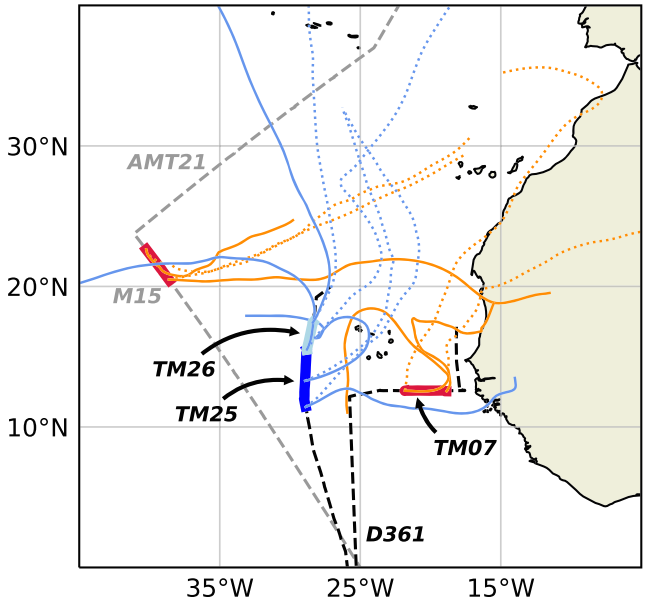

Figure 1. Tracks of the D361 (black) and AMT21 (gray) cruises through the eastern North Atlantic. Aerosol collection periods are indicated by thick solid lines (red for samples with high concentrations of mineral dust, blues for other samples). Five day air mass Back trajectories are shown as dotted lines for arrivals 10 m above the ship's position and solid lines for 1,000 m arrivals. Back trajectories extend beyond the boundaries of the map in some cases.

concentration (Jickells et al., 2016; Shelley et al., 2018), and similar behavior has been observed for Co (Shelley et al., 2018).

In this work, the solubilities of several mineral dust-associated trace elements (Fe, Al, Ti, Mn, Co, and Th) have been examined in size fractionated aerosol samples collected over the tropical Atlantic Ocean. The overall (summed over all size fractions) solubility observed in these samples is compared to that of other non-size fractionated Saharan dust aerosols. Variations in solubility with particle size are discussed in terms of the influences on dust solubility of weathering in source regions and atmospheric processing. The impact of variations in solubility on the suitability of trace elements as proxies for Saharan dust deposition is also considered.

2. Materials and Methods

Size-segregated aerosol samples were collected during two cruises in 2011 in the eastern tropical Atlantic Ocean aboard RRS *Discovery* (Figure 1). Cruise D361 (GEOTRACES section cruise GA06) took place in February–March (Jickells et al., 2016), while D371 (AMT21) crossed the north Atlantic in October as part of the Atlantic Meridional Transect (AMT) program (Baker & Jickells, 2017). Acid-washed Whatman 41 slotted substrates and backup filters were used for trace metal sampling during both cruises (Baker & Jickells, 2017; Jickells et al., 2016). Most aerosol sampling during these cruises was done using Sierra-type cascade impactors to separate the collected material into two size classes, with a boundary at an aerodynamic diameter of ~1 μm. However, the four samples discussed here were collected using multiple impactor stages to give more detailed information on the size distribution of aerosol components (Table 1). Soluble trace metals were extracted from aerosol samples using ammonium acetate solution at pH 4.7 and determined by ICP-OES and ICP-MS. Leaching with ultrapure water was used for major ion (including sodium, nitrate, sulfate, and oxalate) extraction, followed by ion chromatography analysis. The application of these methods to the samples collected during AMT21 and D361 has been described previously (Baker & Jickells, 2017; Bridgestock et al., 2017; Jickells et al., 2016).

The relationship between the solubility of the trace metals in seawater and that determined by the leaching protocol used in this work is unclear, especially for elements other than Fe. The influence of the ammonium acetate leach on the solubility of the D361 and AMT21 samples has been discussed previously (Baker & Jickells, 2017; Jickells et al., 2016); however, the geochemical characteristics and magnitude of solubility are similar to those reported using a number of different leaching solutions, including seawater (Baker et al., 2014; Shelley et al., 2018).

The total metal composition of the multistage samples was determined after a strong acid digestion procedure using 15.4 M HNO_3 (TraceSELECT™, for trace analysis, ≥69.0%, Honeywell Fluka™) and 27–30 M HF (47–51%, Trace Metal™, for Trace Metal Analysis, Fisher Chemical). Portions of each collection substrate were placed in acid-washed Teflon beakers and evaporated gently to dryness after sequential additions of 5 ml HNO_3, 1 ml HF, and 1 ml HNO_3 on a ceramic hotplate (Baker et al., 2006). The hotplate was housed inside a plastic box, which was placed in a fume cupboard. Fumes from the digestion were drawn through a saturated solution of $CaCO_3$ in order to remove any excess HF from the vented air flow. Once digestion was complete, the residues were redissolved in 0.15 M HNO_3, quantitatively transferred to acid-washed 50 ml polypropylene centrifuge tubes and left to stand for 24 hr before filtration through 0.2 μm cartridge filters (cellulose acetate, Sartorius). Blank digestions and digestions of Arizona Test Dust (20–24 mg) were performed with each batch of aerosol digests. Results obtained for Arizona Test Dust are presented in Table 2.

Trace element concentrations in the filtered digests were determined by ICP-MS (iCAP TQ, Thermo Scientific) using rhodium as an internal standard. Calibration solutions were prepared from SPEX

Table 1
Cascade Impactor Stages Used During the D361 and AMT21 Cruises and Their Associated Particle Size Cutoffs (Aerodynamic Diameter) at the Collector Flow Rate Used, 1 m^3 min^{-1}

Impactor stage	Cutoff diameter (μm)
1	7.8
2	3.3
3	1.65
4	1.09
5	0.61
6[a]	0.36

Note. Backup filters (Stage w in Figures 3–5) collected particles smaller than the cutoff for the last impactor stage.
[a]Not used for TM sampling during AMT21.

CertiPrep stock solutions. Certified reference materials (TM27.3 and TMDA64.2, Environment Canada) were analyzed together with each batch of samples. Recoveries for certified elements in these standards were within 5% (Fe, Mn, and Co) and 10% (Al and Ti). Reference values for Th in these CRMs are not available. Blank values and detection limits for impactor stages and backup filters are given in Table S1 in the supporting information.

Fractional solubility for each element was calculated as the ratio of its soluble to total concentration, expressed as a percentage. Separation of aerosol samples into multiple size fractions results in a lower sample loading per stage and hence an increased likelihood of components in individual size fractions being below the limit of detection, particularly when total aerosol trace metal concentrations are low (Sakata et al., 2018). If both soluble and total concentrations were below the detection limit, solubility was not calculated. In cases where either one of the measured values was below detection limit, the detection limit was substituted for the missing value in the calculation. The calculated solubility was therefore an upper limit if the soluble concentration was below detection and a lower limit if the total concentration was below detection. (These maximum and minimum values are indicated by downward and upward pointing arrows, respectively, in Figure 4). Where below detection limit values were present in the calculation of properties summed over sample size fractions (e.g., in Table 3), missing values in the summation were replaced with 75% of the relevant limit of detection. If more than one below detection limit value was present in such a calculation, their contribution to the total was taken to be the square root of the sum of their squares (i.e., they were treated as uncertainties). In order to account for these corrections in the uncertainty in the summed value, for each below detection limit value in a calculation, the associated uncertainty was taken to be 100% of the relevant detection limit.

Air mass back trajectories were calculated for the 5 days prior to sample collection at heights of 10, 500, and 1,000 m above the ship's position using the READY Hysplit archived trajectory model (Draxler & Rolph, 2003).

3. Results and Discussion

3.1. Properties of Size-Fractionated Samples

Two of the samples reported here (AMT21 M15 and D361 TM07) exhibited the orange/brown coloration associated with mineral dust aerosols on several of their upper impactor stages. Air mass back trajectories for these samples (Figure 1) indicated passage of air over regions in Mauritania that have been identified as active dust sources (Stuut et al., 2005). The other samples collected during D361 (TM25 and TM26) did not show dust coloration, had air mass arrivals predominantly from the north, and their total (summed over all size fractions) concentrations of dust-associated trace elements were at least an order of magnitude lower than Samples M15 and TM07 (Table 3). Based on their respective concentrations of soluble Na^+ and total Al, the mass ratios of seaspray to mineral dust in the samples were 0.13 (M15), 0.34 (TM07), 13.2 (TM25), and 6.0 (TM26). Mineral dust was therefore a relatively minor constituent of Samples TM25 and TM26. Isotopic analysis of samples collected concurrently with TM07 and TM25 + TM26 combined also suggests that mineral dust contributed a greater proportion of Pb to Sample TM07 than during the latter period (Bridgestock et al., 2016). Results for the non-dusty samples are reported here, but the focus of this work is on the concentrations and solubility of trace elements in Saharan dust aerosols.

Table 2
Mean and Standard Deviation Elemental Composition of Arizona Test Dust Determined in This Study (n = 5)

Element	Concentration (ppm)
Fe	28,600 ± 1,100
Al	60,300 ± 3,500
Ti	2,510 ± 100
Mn	658 ± 34
Co	15.0 ± 0.5
Th	16.0 ± 0.7

The concentrations of dust-associated elements in Samples M15 and TM07 were within a factor of 2 of each other (Table 3). The lower concentrations observed in Sample M15 may have been partly due to deposition along its probable longer atmospheric transport pathway (M15 was located ~2,200 km west of the coast of Western Sahara, while TM07 was collected ~350 km west of Senegal, although actual

Table 3
Sum of the Total Concentrations of Trace Elements Over All Size Fractions for the Aerosol Samples Considered Here and the Overall Solubility of Those Trace Elements in Each Sample

Sample	Element	Total conc. (pmol m^{-3})	Overall sol. (%)	Element	Total conc. (pmol m^{-3})	Overall sol. (%)
M15	Fe	20,000 ± 130	1.09 ± 0.06	Mn	323 ± 3	43.3 ± 1.6
	Al	74,200 ± 570	2.05 ± 0.07	Co	8.6 ± 0.5	19.0 ± 1.1
	Ti	1,620 ± 14	0.167 ± 0.016	Th	1.85 ± 0.11[a]	6.6 ± 0.4[a]
TM07	Fe	32,800 ± 200	1.08 ± 0.05	Mn	614 ± 5	46.4 ± 0.5
	Al	126,000 ± 1,000	2.04 ± 0.02	Co	15.3 ± 0.8	27.2 ± 1.5
	Ti	2,640 ± 20	0.094 ± 0.005[a]	Th	3.09 ± 0.15[a]	7.9 ± 0.7[a]
TM25	Fe	724 ± 6	2.32 ± 0.26[a]	Mn	22.6 ± 0.3	71.9 ± 1.0
	Al	3,160 ± 50	7.75 ± 0.16	Co	0.43 ± 0.05[a]	29.2 ± 4.0[a]
	Ti	92.1 ± 1.9[a]	<0.139[a]	Th	0.089 ± 0.016[a]	4.9 ± 1.0[a]
TM26	Fe	1,140 ± 6[a]	<0.88[a]	Mn	21.2 ± 0.3	35.2 ± 0.8
	Al	4,600 ± 50	4.23 ± 0.13[a]	Co	0.73 ± 0.06[a]	15.7 ± 1.6[a]
	Ti	98.5 ± 2.0	<0.203[a]	Th	0.14 ± 0.02[a]	3.6 ± 0.8[a]

[a]One or more measurements for individual size fractions were below detection limit. Data for the individual size fractions can be found in Table S2.

transport pathways from source regions will be longer than this). Differences in the relative proportions of dust-associated elements in the different size fractions of these two samples may also be due to changes during transport. For instance, the proportions of total Fe found in the >7.8 μm (Stage 1) and <0.61 μm (Stages w and 6) fractions in TM07 were 13.7% and 9.7% respectively, while the corresponding values for M15 were 5.5% and 26.2%. These differences would be consistent with preferential deposition of larger dust particles during transport (Ryder et al., 2013).

3.2. Solubility-Concentration Relationships of Non-fractionated Dust Aerosols

Figure 2 shows the overall solubility (i.e., the average solubility across all size fractions) of Fe, Al, Ti, Mn, Co, and Th in the samples studied here, together with previously reported data for Saharan dust aerosols collected over the Atlantic Ocean for which soluble element concentrations were determined by the same extraction protocol used here (Jickells et al., 2016). Dust concentration (calculated from total Al concentration, assuming Al to compose 8% of the mass of dust) is plotted on the *x* axes of Figure 2, rather than total element concentration, for convenience. This truncates the range of values on the *x* axes but does not otherwise alter the plots. The data are plotted on both log and linear scales to emphasize the differences in behavior between Fe/Al and Mn ($n = 124$ for these elements). There are fewer observations available for Ti, Co, and Th ($n = 14$), but the latter two elements appear to behave similarly to Mn, with very little variation in solubility with dust (total element) concentration. Shelley et al. (2018) reported that the solubility of Co varied more strongly with total Co concentration in Saharan dust aerosols when ultrapure water was used to leach the soluble element than it did when acetic acid was used as the leaching solution. The data for Ti are rather scattered, and it is not possible to state, based on Figure 2, whether this element's variation in solubility with dust concentration is hyperbolic or less variable. However, Ti has been shown to have a hyperbolic solubility-concentration relationship in other Saharan dust aerosols (Shelley et al., 2018).

3.3. Solubility of Size-Fractionated Samples

Within each of the dusty samples, the distributions of the total concentrations of Fe, Al, Ti, Mn, Co, and Th (as well as P and chromium, not shown) across the size fractions were very similar (Figures 3a and 3b), providing further evidence that dust was the dominant source of these elements in those samples. Although absolute concentrations were much lower (Table 3), total element distributions in Sample TM25 (Figure 3c) were also similar to those in TM07, which may indicate that some dust was present (as hinted at by high-level air mass arrivals from Mauritania early in the collection period, Figure 1). Total element distributions in Sample TM26 indicate higher proportions in particles smaller than ~3 μm (Figure 3d). Broadly similar size distributions of total Fe have been reported in Saharan dust-dominated and northerly marine-influenced aerosol samples in this region of the North Atlantic (Buck et al., 2010).

The size distributions of soluble Mn, Co, and Th in TM07 and M15 are also essentially the same as their total element distributions, but this is not the case for the other soluble elements in these samples (Figures 3e and 3f). In particular, the relative soluble concentrations of Fe and Al were much higher in particles smaller than

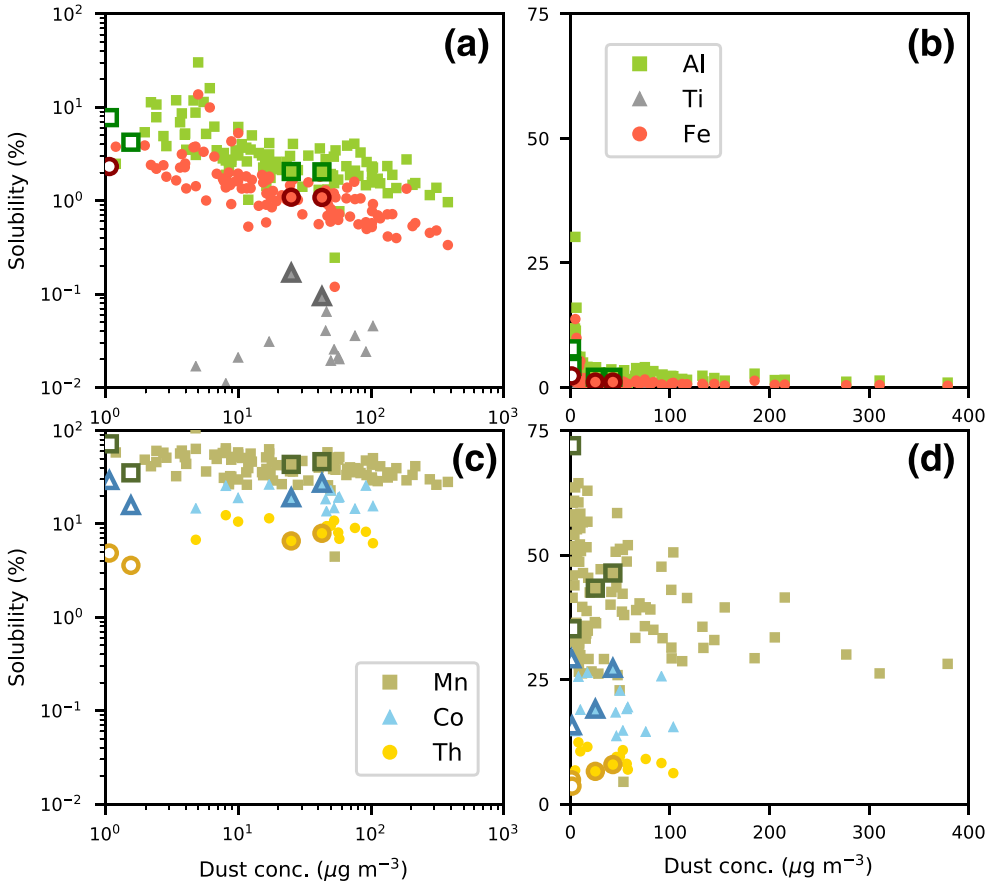

Figure 2. The variation in fractional solubility with atmospheric dust concentration for Fe, Al, and Ti (a, b) and Mn, Co, and Th (c, d) in Saharan dust aerosols sampled over the Atlantic Ocean (Jickells et al., 2016). Values for the size-segregated samples examined in this work (Table 3) are indicated with larger symbols. All other data for Ti, Co, and Th are from D361. (data are plotted on log scales in a and c and linear scales in b and d).

~1.65 μm (Stages w to 4) than were their relative total concentrations. Due to their much lower overall concentrations, soluble concentrations in Samples TM25 and TM26 were not always detectable. (Below detection limit, concentrations are not plotted in Figures 3g and 3h for clarity, but all relevant values are included in Table S1). Partly because the size distributions of the elements' total concentrations were less uniform than for the dusty samples, and partly because there was less data available for the soluble elements, it is difficult to discern whether Fe and Al soluble concentrations are enhanced in the finer fractions of the non-dusty samples.

As a result of the differences in the soluble concentrations, there are some striking differences in the variation of fractional solubility across the aerosol size distribution for the two groups of elements (Figure 4). The profiles of Mn, Co, and Th solubility are relatively flat across the size range, while those of Fe, Al, and Ti show distinct maxima in the smaller size fractions, especially for the dusty samples. Buck et al. (2010) have also reported that the solubility of Fe was higher in particles in the ~0.3–1 μm size range than in larger (>~3 μm) particles in dust-dominated aerosols over the tropical Atlantic, and Ooki et al. (2009) reported higher Fe solubility (up to 12%) in fine (<3.3 μm) fractions of Asian mineral dust aerosol collected at Hokkaido, Japan.

3.4. Influences on Dust Solubility

The enhancement of solubility in fine dust fractions for Fe, Al, and Ti, and the absence of such enhancement for Mn, Co, and Th (Figures 4a, 4b, 4e, and 4f), is intriguing, especially since these groups of elements are the same as those which do, and do not, exhibit hyperbolic changes in overall solubility with changing

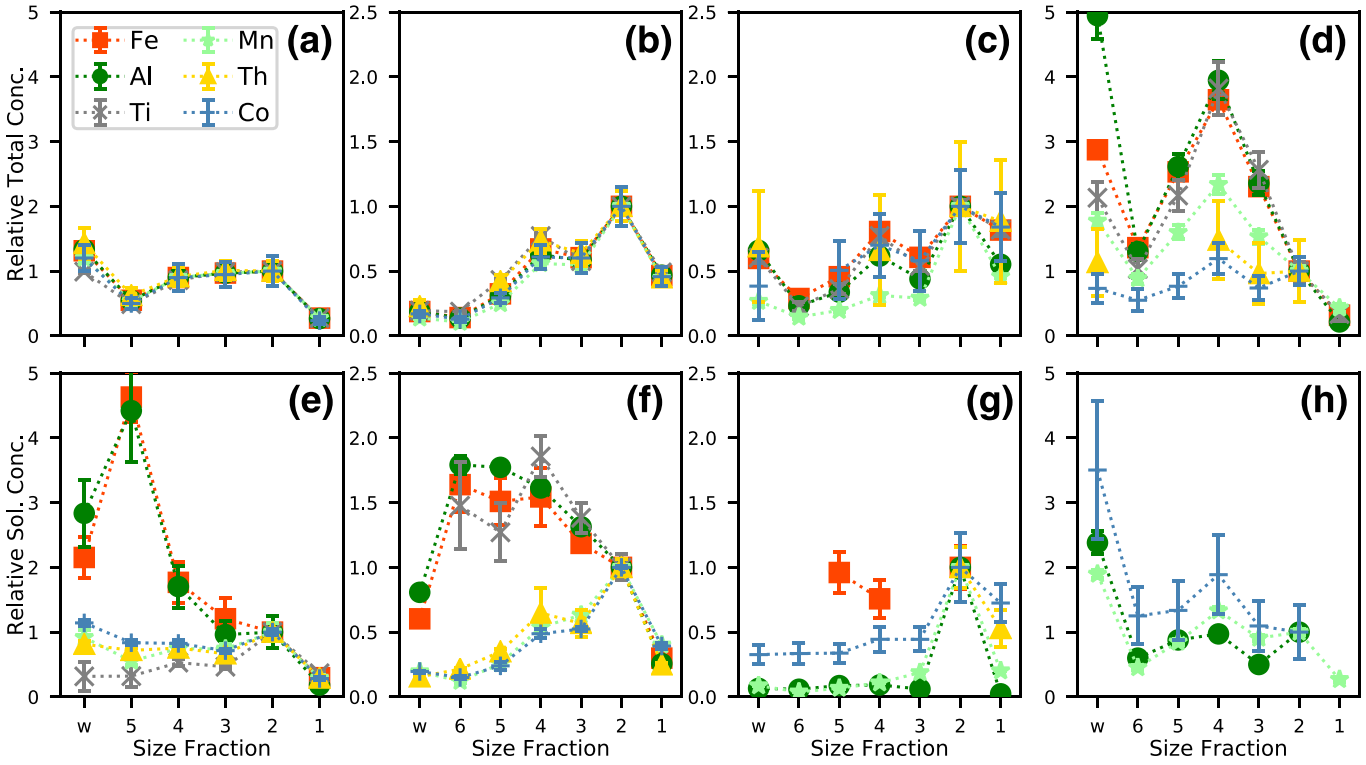

Figure 3. Concentrations of total (a–d) and soluble (e–h) elements in each aerosol size fraction normalized to their respective concentrations in impactor Stage 2 for samples M15 (a, e), TM07 (b, f), TM25 (c, g), and TM26 (d, h). (numbers on *x* axis refer to the cascade impactor stages (Table 1) and *w* to the backup filter).

atmospheric dust (and total element) concentrations (Figure 2). A variety of proposed mechanisms could potentially account for the observed solubility-total atmospheric concentration behavior: mixing of dust with fine, high-solubility anthropogenic aerosol (as suggested for Fe (Sedwick et al., 2007; Sholkovitz et al., 2009)); acid processing of dust particles during atmospheric transport (Spokes et al., 1994); and preferential removal of larger particles during atmospheric transport and consequent shift to a dust population with a higher surface area to volume ratio (Baker & Jickells, 2006).

The information available from the samples studied here is insufficient to determine unambiguously whether any one of these mechanisms dominates their solubility behavior. If inclusion of anthropogenic Fe makes a significant contribution to the solubility of Samples TM07 and M15, then similar high-solubility anthropogenic sources of Al (and Ti) would also be required to account for the observed solubility in these samples. This seems unlikely but cannot be discounted without further evidence on anthropogenic emissions of the latter elements. Changes in mineral particle size distribution with transport cannot account for the particle size-dependent variation of solubility within each sample.

Acid processing provides a plausible mechanism which could be responsible for the similar enhancement of Fe, Al, and Ti solubility in the fine fractions of Samples TM07 and M15. Figure 5 shows the distributions of the major acid species (nitrate, non-seasalt sulfate, and oxalate) in all of the aerosol samples. Nitrate was present predominantly on the larger size fractions, most probably as a result of the uptake of HNO_3 into seasalt particles and the subsequent displacement of HCl (Andreae & Crutzen, 1997). Thus, acidity arising from nitrate probably does not play a role in the enhancement of Fe and Al solubility in the finer fractions of the dusty samples. The size distributions of nss-SO_4^{2-} show higher concentrations in the finer fractions, although there were noticeably higher proportions in the larger size fractions in the dusty samples (Figures 5a and 5b). The >1 μm size fractions accounted for 42%, 56%, 10%, and 20% of total nss-SO_4^{2-} in Samples M15, TM07, TM25, and TM26, respectively. These distributions might be a result of the higher particle surface area available for SO_2 uptake when dust is present in high concentrations. Fang et al. (2017)

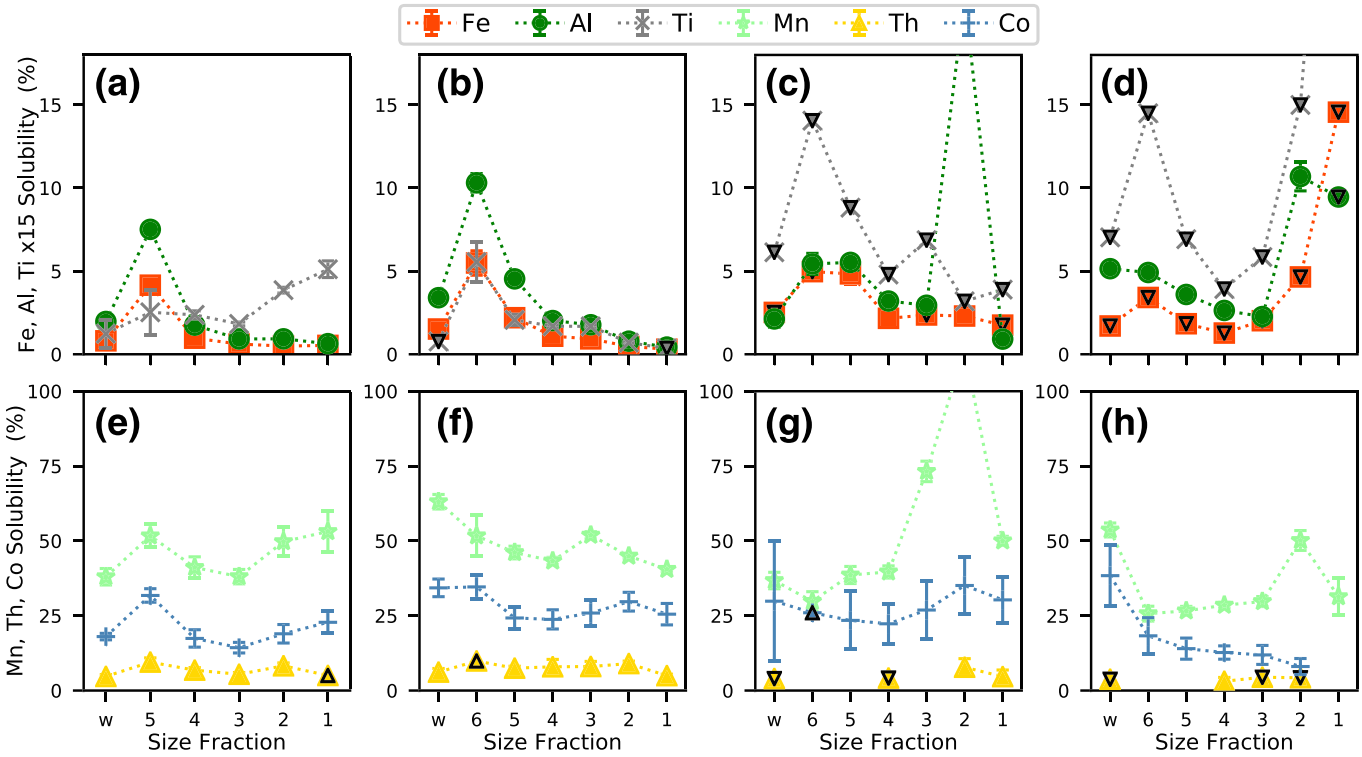

Figure 4. Fractional solubility (%) of elements in each aerosol size fraction for Samples M15 (a, e), TM07 (b, f), TM25 (c, g), and TM26 (d, h). Ti solubility is increased 15-fold for clarity. Upward and downward pointing triangles on individual markers indicate that the plotted values are minima or maxima, respectively. Size fractions are as described in Figure 3.

found SO_4^{2-} predominantly in fine (~0.1–10 μm) particles and total Cu and Fe in coarser (~0.7–20 μm) particles in urban aerosols and reported enhanced solubility of Cu and Fe in aerosol size fractions where the SO_4^{2-} and total Cu/Fe populations overlapped (~0.7–8 μm). This change in solubility appeared to be linked to a large change in pH between the <2.5 μm aerosol (pH < 2) and the coarser fractions (pH > 6) and resulted in the soluble metals being distributed on smaller particles than their total metals (Fang et al., 2017), as is observed for Fe, Al, and Ti in the dusty samples here. Similar dependence on pH changes driven by the distribution of nss-SO_4^{2-} may be responsible for the enhanced solubility of Fe, Al, and Ti observed in Samples M15 and TM07. Interestingly, Fang et al. (2017) also reported that there was much less difference between the size distributions of soluble and total Mn than for Cu and Fe. Although complexation with oxalate can stabilize dissolved Fe (Paris et al., 2011), the distribution of oxalate does not appear to be related to the enhanced concentrations of soluble Fe in the dusty samples.

Whatever the cause of the higher solubility of Fe, Al, and Ti in the fine fractions of the dusty samples, it is apparent that it does not result in similar enhancement in the solubility of Mn, Co, and Th (Figures 4e and 4f). Weathering in arid environments produces mineral phases that have quite distinct geochemical compositions that are enriched in Mn, such as desert varnishes (Potter & Rossman, 1979), and these phases have been found coating Saharan dust particles collected at Barbados (Rydell & Prospero, 1972). Manganese oxides in soils are also noted to be associated with Co (Krauskopf & Bird, 1995). If Mn-enriched weathering products are present in Saharan dust aerosols, their size distribution appears to be similar to those of the principal Fe-, Al-, and Ti- bearing minerals, as indicated by the similarity in the size distributions of the total concentrations of all of the trace metals (Figures 3a and 3b). Whether such Mn-enriched minerals are associated with Co and Th, and how their dissolution behavior differs from that of Fe-bearing minerals, is a subject for further study. Although Th solubility in a small number of other Saharan dust aerosol samples has been reported (Anderson et al., 2016), there does not appear to be any data, other than that reported here, with which to assess the variation of Th solubility with dust concentration changes during atmospheric transport. However, the similarity in the behavior of Mn and Th reported here suggests that the fractional

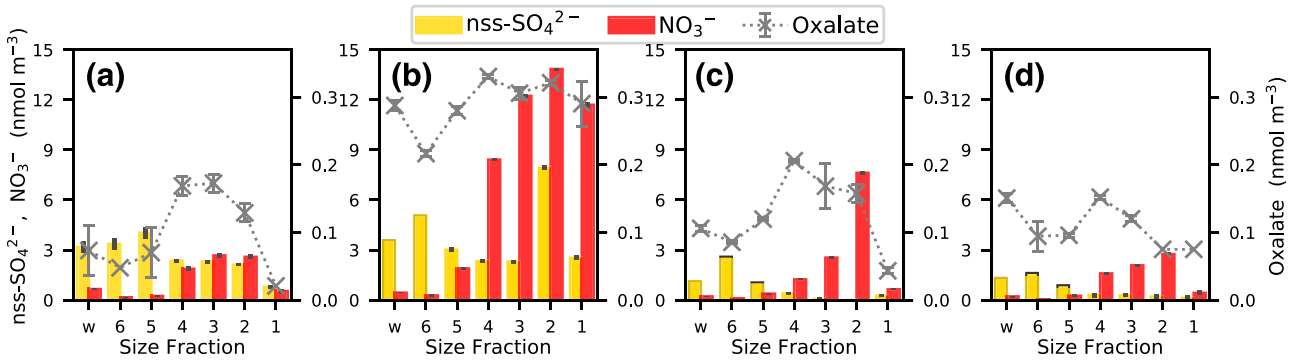

Figure 5. Concentrations of non-seasalt sulfate, nitrate, and oxalate in each aerosol size fraction for Samples M15 (a), TM07 (b), TM25 (c), and TM26 (d). Black caps on nss-SO_4^{2-} concentration bars (e.g., Stages 5 and 6 in d)) indicate the uncertainty due to Na^+ concentrations being undetectable. Size fractions are as described in Figure 3.

solubility of Th over large gradients in dust concentration might be relatively constant. This would simplify the use of seawater Th concentration as a proxy for dust deposition flux (Hsieh et al., 2011), by reducing uncertainties in this term with respect to proxies (such as Al) that have hyperbolic solubility-concentration relationships. The small number of observations of Th solubility in aerosols (13 bulk values (Jickells et al., 2016, Figure 2), ~15 bulk samples (Anderson et al., 2016), 2 size-fractionated samples (this work)) suggests that further work is necessary to improve the use of Th as a dust proxy.

4. Conclusions

Separation of two Saharan dust aerosol samples collected over the tropical Atlantic Ocean into multiple size fractions has demonstrated that the two groups of dust-associated trace metals (Fe, Al, Ti and Mn, Co, Th) show very different solubility characteristics in the particle size range 0.61–3.3 μm. The former group (Fe, Al, and Ti) have enhanced solubility in this size range while the latter (Mn, Co, and Th) do not. The solubility of these two groups also differs over large gradients in their total atmospheric concentration (as Saharan dust is transported over long distances in the atmosphere). The presence of Mn-enriched mineral phases in desert soils, and the association of Co with Mn minerals, might go some way to explain the differences in solubility between these two groups of elements and the unusual behavior of Mn, Co, and Th solubility in Saharan dust aerosols during atmospheric transport (Jickells et al., 2016; Shelley et al., 2018). It should be noted, however, that further work is necessary to confirm the variations in trace element solubility with particle size and total atmospheric concentration reported here due to the small size of the currently available data set, especially for Ti, Co, and Th.

Acknowledgments

This work was supported by the UK Natural Environment Research Council, through Grant NE/H00548X/1 (UK GEOTRACES) and NE/F017359/1, and the University of East Anglia. The Atlantic Meridional Transect is funded by the UK Natural Environment Research Council through its National Capability Long-term Single Centre Science Programme, Climate Linked Atlantic Sector Science (Grant NE/R015953/1). This study contributes to the international IMBeR project and is contribution number 350 of the AMT programme. We thank Eric Achterberg and Glen Tarran, chief scientists of the D361 and AMT21 cruises, Chan Yodle for collection of the AMT21 samples and analysis of major ions in Sample M15, and the Masters and crews of RRS *Discovery*. We gratefully acknowledge the NOAA Air Resources Laboratory (ARL) for the provision of the HYSPLIT transport and dispersion model and READY website (http://www.arl.noaa.gov/ready.html) used in this publication. The authors declare that they have no conflict of interest. The data used in this publication are available from the British Oceanographic Data Centre (https://www.bodc.ac.uk/projects/data_management/uk/amt/data_delivery/(AMT21) and https://www.bodc.ac.uk/geotraces/ (D361)) and the SOLAS Aerosol and Rain Composition database (https://www.bodc.ac.uk/solas_integration/implementation_products/group1/aerosol_rain/). We thank Morgane Perron and an anonymous reviewer for their helpful and constructive comments on the manuscript. The authors declare that they have no competing financial interests.

References

Aguilar-Islas, A. M., Wu, J. F., Rember, R., Johansen, A. M., & Shank, L. M. (2010). Dissolution of aerosol-derived iron in seawater: Leach solution chemistry, aerosol type, and colloidal iron fraction. *Marine Chemistry*, *120*(1–4), 25–33. https://doi.org/10.1016/j.marchem.2009.01.011

Anderson, R. F., Cheng, H., Edwards, R. L., Fleisher, M. Q., Hayes, C. T., Huang, K.-F., et al. (2016). How well can we quantify dust deposition to the ocean? *Philosophical Transactions A*, *374*(2081), 20150285. https://doi.org/10.1098/rsta.2015.0285

Andreae, M. O., & Crutzen, P. J. (1997). Atmospheric aerosols: Biogeochemical sources and role in atmospheric chemistry. *Science*, *276*(5315), 1052–1058. https://doi.org/10.1126/science.276.5315.1052

Baker, A. R., & Jickells, T. D. (2006). Mineral particle size as a control on aerosol iron solubility. *Geophysical Research Letters*, *33*, L17608. https://doi.org/10.1029/2006GL026557

Baker, A. R., & Jickells, T. D. (2017). Atmospheric deposition of soluble trace elements along the Atlantic Meridional transect (AMT). *Progress in Oceanography*, *158*, 41–51. https://doi.org/10.1016/j.pocean.2016.10.002

Baker, A. R., Jickells, T. D., Witt, M., & Linge, K. L. (2006). Trends in the solubility of iron, aluminium, manganese and phosphorus in aerosol collected over the Atlantic Ocean. *Marine Chemistry*, *98*(1), 43–58. https://doi.org/10.1016/j.marchem.2005.06.004

Baker, A. R., Laskina, O., & Grassian, V. H. (2014). Processing and ageing in the atmosphere. In P. Knippertz & J. B. Stuut (Eds.), *Mineral dust: A key player in the Earth system* (pp. 75–92). Dordrecht: Springer.

Bridgestock, L., Rehkämper, M., Van de Flierdt, T., Murphy, K., Khondoker, R., Baker, A. R., et al. (2017). The Cd isotope composition of atmospheric aerosols from the tropical Atlantic Ocean. *Geophysical Research Letters*, *44*, 2932–2940. https://doi.org/10.1002/2017GL072748

Bridgestock, L., van de Flierdt, T., Rehkämper, M., Paul, M., Middag, R., Milne, A., et al. (2016). Return of naturally sourced Pb to Atlantic surface waters. *Nature Communications*, *7*(1), 12,921. https://doi.org/10.1038/ncomms12921

Buck, C. S., Landing, W. M., & Resing, J. A. (2010). Particle size and aerosol iron solubility: A high-resolution analysis of Atlantic aerosols. *Marine Chemistry*, *120*(1–4), 14–24. https://doi.org/10.1016/j.marchem.2008.11.002

Chen, Y., & Siefert, R. L. (2004). Seasonal and spatial distributions and dry deposition fluxes of atmospheric total and labile iron over the tropical and subtropical North Atlantic Ocean. *Journal of Geophysical Research*, *109*, D09305. https://doi.org/10.1029/2003jd003958

Draxler, R. R., & Rolph, G. D. (2003). *HYSPLIT (HYbrid Single-Particle Lagrangian Integrated Trajectory) Model access via NOAA ARL READY Website*. New York: NOAA Air Resources Laboratory. Retrieved from Silver Spring, MD: http://www.arl.noaa.gov/ready/hysplit4.html

Fang, T., Guo, H., Zeng, L., Verma, V., Nenes, A., & Weber, R. J. (2017). Highly acidic ambient particles, soluble metals, and oxidative potential: A link between sulfate and aerosol toxicity. *Environmental Science & Technology*, *51*(5), 2611–2620. https://doi.org/10.1021/acs.est.6b06151

Hsieh, Y. T., Henderson, G. M., & Thomas, A. L. (2011). Combining seawater ^{232}Th and ^{230}Th concentrations to determine dust fluxes to the surface ocean. *Earth and Planetary Science Letters*, *312*(3–4), 280–290. https://doi.org/10.1016/j.epsl.2011.10.022

Jickells, T. D., An, Z. S., Anderson, K. K., Baker, A. R., Bergametti, G., Brooks, N., et al. (2005). Global iron connections between desert dust, ocean biogeochemistry and climate. *Science*, *308*(5718), 67–71. https://doi.org/10.1126/science.1105959

Jickells, T. D., Baker, A. R., & Chance, R. (2016). Atmospheric transport of trace elements and nutrients to the oceans. *Philosophical Transactions of the Royal Society of London, Series A: Mathematical, Physical and Engineering Sciences*, *374*(2081), 20150286. https://doi.org/10.1098/rsta.2015.0286

Krauskopf, K. B., & Bird, D. K. (1995). *Introduction to geochemistry*. New York: McGraw-Hill Inc.

Mahowald, N. M., Hamilton, D. S., Mackey, K. R. M., Moore, J. K., Baker, A. R., Scanza, R. A., & Zhang, Y. (2018). Aerosol trace metal leaching and impacts on marine microorganisms. *Nature Communications*, *9*(1), 2614. https://doi.org/10.1038/s41467-018-04970-7

Measures, C. I., Sato, T., Vink, S., Howell, S., & Li, Y. H. (2010). The fractional solubility of aluminium from mineral aerosols collected in Hawaii and implications for atmospheric deposition of biogeochemically important trace elements. *Marine Chemistry*, *120*(1–4), 144–153. https://doi.org/10.1016/j.marchem.2009.01.014

Morel, F. M. M., Kustka, A. B., & Shaked, Y. (2008). The role of unchelated Fe in the iron nutrition of phytoplankton. *Limnology and Oceanography*, *53*(1), 400–404. https://doi.org/10.4319/lo.2008.53.1.0400

Ooki, A., Nishioka, J., Ono, T., & Noriki, S. (2009). Size dependence of iron solubility of Asian mineral dust particles. *Journal of Geophysical Research*, *114*, D03202. https://doi.org/10.1029/2008jd010804

Paris, R., Desboeufs, K. V., & Journet, E. (2011). Variability of dust iron solubility in atmospheric waters: Investigation of the role of oxalate organic complexation. *Atmospheric Environment*, *45*(36), 6510–6517. https://doi.org/10.1016/j.atmosenv.2011.08.068

Potter, R. M., & Rossman, G. R. (1979). The manganese- and iron-oxide mineralogy of desert varnish. *Chemical Geology*, *25*(1–2), 79–94. https://doi.org/10.1016/0009-2541(79)90085-8

Prospero, J. M., Nees, R. T., & Uematsu, M. (1987). Deposition rate of particulate and dissolved aluminum derived from Saharan dust in precipitation at Miami, Florida. *Journal of Geophysical Research*, *92*(D12), 14723–714,731. https://doi.org/10.1029/JD092iD12p14723

Rydell, H. S., & Prospero, J. M. (1972). Uranium and thorium concentrations in wind-borne Saharan dust over western equatorial North Atlantic Ocean. *Earth and Planetary Science Letters*, *14*(3), 397–402. https://doi.org/10.1016/0012-821X(72)90140-9

Ryder, C. L., Highwood, E. J., Lai, T. M., Sodemann, H., & Marsham, J. H. (2013). Impact of atmospheric transport on the evolution of microphysical and optical properties of Saharan dust. *Geophysical Research Letters*, *40*, 2433–2438. https://doi.org/10.1002/grl.50482

Sakata, K., Kurisu, M., Tanimoto, H., Sakaguchi, A., Uematsu, M., Miyamoto, C., & Takahashi, Y. (2018). Custom-made PTFE filters for ultra-clean size-fractionated aerosol sampling for trace metals. *Marine Chemistry*, *206*, 100–108. https://doi.org/10.1016/j.marchem.2018.09.009

Sedwick, P. N., Sholkovitz, E. R., & Church, T. M. (2007). Impact of anthropogenic combustion emissions on the fractional solubility of aerosol iron: Evidence from the Sargasso Sea. *Geochemistry, Geophysics, Geosystems*, *8*, Q10Q06. https://doi.org/10.1029/2007gc001586

Shelley, R. U., Landing, W. M., Ussher, S. J., Planquette, H., & Sarthou, G. (2018). Regional trends in the fractional solubility of Fe and other metals from North Atlantic aerosols (GEOTRACES cruises GA01 and GA03) following a two-stage leach. *Biogeosciences*, *15*(8), 2271–2288. https://doi.org/10.5194/bg-15-2271-2018

Sholkovitz, E. R., Sedwick, P. N., & Church, T. M. (2009). Influence of anthropogenic combustion emissions on the deposition of soluble aerosol iron to the ocean: Empirical estimates for island sites in the North Atlantic. *Geochimica et Cosmochimica Acta*, *73*(14), 3981–4003. https://doi.org/10.1016/j.gca.2009.04.029

Sholkovitz, E. R., Sedwick, P. N., Church, T. M., Baker, A. R., & Powell, C. F. (2012). Fractional solubility of aerosol iron: Synthesis of a global-scale data set. *Geochimica et Cosmochimica Acta*, *89*, 173–189. https://doi.org/10.1016/j.gca.2012.04.022

Spokes, L. J., Jickells, T. D., & Lim, B. (1994). Solubilisation of aerosol trace metals by cloud processing: A laboratory study. *Geochimica et Cosmochimica Acta*, *58*(15), 3281–3287. https://doi.org/10.1016/0016-7037(94)90056-6

Stuut, J. B., Zabel, M., Ratmeyer, V., Helmke, P., Schefuss, E., Lavik, G., & Schneider, R. (2005). Provenance of present-day eolian dust collected off NW Africa. *Journal of Geophysical Research*, *110*, D04202. https://doi.org/10.1029/2004jd005161